



HAL
open science

Cortical-layer-specific effects of PACAP and tPA on interneuron migration during post-natal development of the cerebellum

Emilie Raoult, Magalie Bénard, Hitoshi Komuro, Alexis Lebon, Denis Vivien,
Alain Fournier, Hubert Vaudry, David Vaudry, Ludovic Galas

► To cite this version:

Emilie Raoult, Magalie Bénard, Hitoshi Komuro, Alexis Lebon, Denis Vivien, et al.. Cortical-layer-specific effects of PACAP and tPA on interneuron migration during post-natal development of the cerebellum. *Journal of Neurochemistry*, 2014, 130 (2), pp.241-254. 10.1111/jnc.12714 . hal-01196821

HAL Id: hal-01196821

<https://hal.science/hal-01196821>

Submitted on 10 Sep 2015

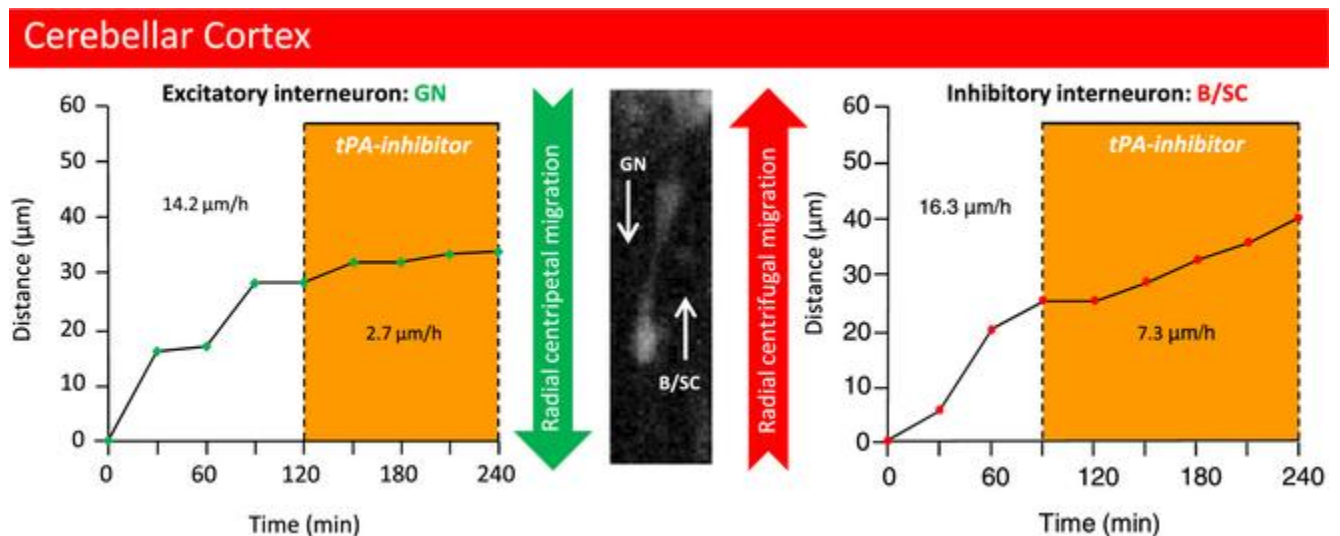
HAL is a multi-disciplinary open access archive for the deposit and dissemination of scientific research documents, whether they are published or not. The documents may come from teaching and research institutions in France or abroad, or from public or private research centers.

L'archive ouverte pluridisciplinaire **HAL**, est destinée au dépôt et à la diffusion de documents scientifiques de niveau recherche, publiés ou non, émanant des établissements d'enseignement et de recherche français ou étrangers, des laboratoires publics ou privés.

Cortical-layer-specific effects of PACAP and tPA on interneuron migration during post-natal development of the cerebellum

Emilie Raoul^{1,2,3,4,†},
Magalie Bénard^{1,2,†},
Hitoshi Komuro⁵,
Alexis Lebon^{1,2,3,4},
Denis Vivien⁶,
Alain Fournier^{4,7},
Hubert Vaudry^{1,2,3,4},
David Vaudry^{1,2,3,4} and
Ludovic Galas^{1,2,7}

Abstract



During early post-natal development of the cerebellum, granule neurons (GN) execute a centripetal migration toward the internal granular layer, whereas basket and stellate cells (B/SC) migrate centrifugally to reach their final position in the molecular layer (ML). We have previously shown that pituitary adenylate cyclase-activating polypeptide (PACAP) stimulates *in vitro* the expression and release of the serine protease tissue-type plasminogen activator (tPA) from GN, but the coordinated role of PACAP and tPA during interneuron migration has not yet been investigated. Here, we show that endogenous PACAP is responsible for the transient arrest phase of GN at the level of the Purkinje cell layer (PCL) but has no effect on B/SC. tPA is devoid of direct effect on GN motility *in vitro*, although it is widely distributed along interneuron migratory routes in the ML, PCL, and internal granular layer. Interestingly, plasminogen activator inhibitor 1 reduces the migration speed of GN in the ML and PCL, and that of B/SC in the ML. Taken together, these

results reveal for the first time that tPA facilitates the migration of both GN and fast B/SC at the level of their intersection in the ML through degradation of the extracellular matrix.

Crucial role of tissue plasminogen activator (tPA) in interneuron migration. Interneuron migration is a critical step for normal establishment of neuronal network. This study indicates that, in the post-natal cerebellum, tPA facilitates the opposite migration of immature excitatory granule neurons (GN) and immature inhibitory basket/stellate cells (B/SC) along the same migratory route. These data show that tPA exerts a pivotal role in neurodevelopment.

During brain development, the migration of immature neurons from germinative zones to their final destination is essential for the establishment of proper neuronal circuits (Rakic [1990](#); Hatten [1999](#); Komuro and Yacubova [2003](#); Evsyukova *et al.* [2013](#)). Impairment of this process results in either cell death or misplacement of the neurons, leading to deficiency of diverse brain functions (Rakic [1988](#); Flint and Kriegstein [1997](#); Gressens [2006](#)). In the developing cerebellum, immature granule neurons (GN; excitatory interneurons) and basket/stellate cells (B/SC; inhibitory interneurons) originate from two separate germinative zones, and exhibit distinct modes of migration over the same developmental period *that is*, the first three post-natal weeks (Komuro and Yacubova [2003](#); Consalez and Hawkes [2013](#)). Thus, upon completion of their final mitosis, GN migrate tangentially within the external granular layer (EGL) and then change direction to migrate radially along the processes of Bergmann glial cells through the molecular layer (ML) (Komuro and Rakic [1998](#), Komuro *et al.* [2001](#)). When entering the Purkinje cell layer (PCL), GN detach from glial cells and slow down (Komuro and Rakic [1998](#)). Two hours later, GN resume their migration and cross the border between the PCL and the internal granular layer (IGL). Within the IGL, GN migrate radially until reaching their final position at the bottom of the IGL (Komuro and Rakic [1998](#)). In contrast to GN, less is known about B/SC migration but they exhibit a centrifugal move during early post-natal development from the deep white matter to the ML (Zhang and Goldman [1996](#); Milosevic and Goldman [2004](#)) where they complete their migration in four phases (Cameron *et al.* [2009a](#)).

Pituitary adenylate cyclase-activating polypeptide (PACAP) is a 38-amino acid neuropeptide whose primary structure has been remarkably well conserved during evolution (Vaudry *et al.* [2000](#)). PACAP belongs to a family of structurally related peptides, comprising secretin, glucagon, vasoactive intestinal polypeptide, peptide histidine-isoleucine, growth hormone-releasing hormone, and helodermin (Vaudry *et al.* [2009](#)). In the post-natal cerebellum of rodents, PACAP is expressed sporadically at the bottom of the ML, intensively in the PCL, and throughout the IGL (Nielsen *et al.* [1998](#); Hannibal [2002](#); Cameron *et al.* [2007](#)). *In vitro* and *in vivo* studies have shown that PACAP exerts an inhibitory effect on GN migration (Falluel-Morel *et al.* [2005](#); Cameron *et al.* [2007](#)). In particular, endogenous PACAP is responsible for the transient arrest phase in the PCL that lasts for approximately 2 h (Cameron *et al.* [2007](#)). Recently, PACAP has been shown to stimulate *in vitro* the expression and release of tissue-type plasminogen activator (tPA) which contributes to the neuroprotective effect of PACAP on GN (Raoult *et al.* [2011](#)). tPA is an extracellular serine protease that

converts the proenzyme plasminogen into the active protease plasmin, which in turn degrades extracellular matrix (EM) components such as cell adhesion molecules or laminin (Garcia-Rocha *et al.* [1994](#); Yepes and Lawrence [2004](#)). tPA-induced proteolysis and endogenous protease inhibitors, including plasminogen activator inhibitor-1 (PAI-1), are known to play key roles in neuritogenesis, neuronal plasticity, and death (Melchor and Strickland [2005](#)). Interestingly, during development of the post-natal cerebellum, tPA is detected in leading processes of GN (Krystosek and Seeds [1981a,b](#); Seeds *et al.* [1997](#)) and facilitates GN migration (Seeds *et al.* [1999](#)). The developing cerebellum of tPA-deficient mice exhibits an increased number of GN in transit within the ML as a result of a decrease in neuronal migration speed (Seeds *et al.* [1999](#)). As a matter of fact, plasminogen mRNA is widely expressed in the cerebellar EGL, ML, and IGL of newborn mice (Basham and Seeds [2001](#)).

Centripetal GN and centrifugal B/SC migration may involve different mechanisms, such as chemotactism or EM degradation, to guide the cells. Several molecules which affect the velocity of GN have already been identified (Cameron *et al.* [2009b](#)), but the exact mechanisms involved in the control of cell migration in each cortical layer are still largely unknown. Furthermore, no factor regulating B/SC movement during brain development has so far been identified (Cameron *et al.* [2009b](#)). Thus, the aim of this study was to determine a possible role of PACAP, tPA, and PACAP-induced tPA release in the centripetal GN and centrifugal B/SC migrations in the rat cerebellar cortical layers



Materials and methods

Reagents and drugs

Poly-D-Lysine, poly-L-Lysine, laminin, and antibiotic-antimycotic solution were purchased from Sigma-Aldrich (Saint-Quentin Fallavier, France). Dulbecco's modified Eagle's medium, Ham's F12, Hank's buffered salt solution, bovine serum albumin (BSA), and N-2 supplement were from Fisher Scientific (Illkirch, France). The 38-amino acid form of PACAP (PACAP38) and the PACAP antagonist (PACAP6-38) were synthesized as previously described (Bourgault *et al.* [2009](#)). tPA, PAI-1, and plasminogen were obtained from Calbiochem (Meudon, France) and applied at a concentration of 10^{-7} M according to previous reports (Raoult *et al.* [2011](#); Li *et al.* [2013](#)).

Animals

Animals (male or female Wistar rats) were born and bred in an accredited animal facility (approval B.76-451-04), according to the French guide for the care and use of laboratory animals. Experiments were conducted under the supervision of authorized investigators (M.B., L.G., D.V., and H.V.) in accordance with the European Community Council Directive (2010/63/UE of September 22, 2010) and the French Ministry of Agriculture.

Microexplants

Microexplants were prepared from P2–P4 Wistar rat cerebella as previously described (Raoult *et al.* [2011](#)). Transmitted light imaging of GN was performed using an incubation chamber (37°C and 95% O₂, 5% CO₂) fixed to the stand of an inverted microscope (IRE2; Leica Microsystems, Nanterre, France), with a ×16 oil-immersion objective (NA = 0.5). Images of migrating GN were collected every minute for 3 h. Data were analyzed using the Metamorph software (Roper Scientific, Evry, France).

Immunohistochemistry

After deep anesthesia (intraperitoneal injection of 400 mg/kg chloral hydrate), 10-day-old Wistar rats were perfused transcardially with phosphate-buffered saline (PBS; pH 7.4), followed by 4% paraformaldehyde in PBS. Brains were quickly dissected and post-fixed overnight at 4°C with the same fixative solution. Tissues were stored for 24 h in a solution of PBS containing 15% and 30% sucrose, successively. Thereafter, tissues were cut at a thickness of 12 µm in the sagittal plane with a cryostat (CM 3050 S, Leica Microsystems). Tissue slices were mounted on glass slides coated with 0.5% gelatin and 5% chrome alun. After a 30-min exposure with 1% BSA in PBS, the tissue sections were incubated for 2 h at 22°C with an antiserum raised in mouse against tPA (1 : 200, Abnova; Millipore, Molsheim, France) or/and an antiserum raised in rabbit against calbindin (1 : 500, Abnova; Millipore) containing 0.3% Triton X-100 and 1% BSA in PBS. The sections were rinsed in three successive baths of PBS and incubated for 2 h at 22°C with Alexa 488-conjugated goat anti-mouse (1 : 200; Invitrogen, Carlsbad, CA, USA) or/and Alexa 594-conjugated donkey anti-rabbit (1 : 200; Invitrogen) containing 0.3% Triton X-100 and 1% BSA in PBS. The sections were then rinsed with PBS (three times) and labeled for 1 min with 4'6-diamidino-2-phenylindole (DAPI, 2 µg/mL) for nuclei counter-staining. After rinsing with PBS, the sections were mounted in PBS/glycerol (1 : 1, v/v). The preparations were examined on a Leica SP2 upright confocal laser scanning microscope (DM RXA-UV) equipped with Acousto-Optical Beam Splitter system (Leica Microsystems). For confocal images, DAPI, Alexa 488, and Alexa 594 were excited respectively at 405, 488, and 594 nm and fluorescence signals were collected through the sequential mode.

Interneuron migration in acute slice preparations

Cerebella of 10-day-old Wistar rats were sectioned in the sagittal plane into 180 µm-thick slices with a vibrating blade microtome (VT1000S, Leica Microsystems) (Kumada and Komuro [2004](#); Cameron *et al.* [2007](#)). To label interneurons, cerebellar slices were incubated for 5 min in 10 µM Cell Tracker Green (CTG) (Invitrogen), which was added to the culture medium. The culture medium was composed of Dulbecco's modified Eagle's medium/Ham's F12 with 1% N-2 supplement and 1% antibiotic-antimycotic solution (Sigma-Aldrich). The slices were subsequently washed with culture medium, placed onto a polyester membrane insert from a 6-well plate and incubated in a 5% CO₂ atmosphere. Two to six hours after labeling, slices were transferred into an incubator attached to the stand of a confocal microscope (TCS LSI, Leica Microsystems). The temperature of the chamber was kept at 37.0 ± 0.5°C

using a temperature controller (Tempcontrol 37-2 digital 2-channel; PeCon, Ulm, Germany), and the slices were supplied with constant gas flow (95% O₂, 5% CO₂; CO₂-controller, PeCon). To visualize interneuron migration in the tissue slices, the preparation was illuminated with a 488-nm wavelength light by means of a laser diode through a confocal laser scanning microscope equipped with a x2 dry objective (working distance: 39 mm, diameter: 58 mm, Leica Microsystems), and fluorescence emission was detected from 500 to 530 nm. To finely resolve the movement of interneurons, images were acquired with an additional optical zoom factor of 1.5 to 2.0. Images of GN in a single focal plane or up to 10 different focal planes along the z-axis were collected every 30 min for up to 5 h. Distinction of CTG-labeled GN and basket and stellate cell (B/SC) were based on their centripetal and centrifugal radial migration, respectively. For this reason, GN migration was studied in the ML, PCL, and IGL, whereas B/SC analysis was restricted to the ML. As immature basket and stellate cells cannot be morphologically distinguished, they were collectively identified as BS/C. Data were analyzed using ImageJ (NIH).

Statistical analysis

All data are expressed as the mean ± SEM value from three to seven independent experiments. Statistical analyses were conducted using a Kruskal–Wallis test or by the Mann–Whitney test using PRISM software (GraphPad Software, San Diego, CA, USA).

Results

Effect of PACAP, tPA, PAI-1, and plasminogen on isolated rat GN

Using microexplant cultures from P2 to P4 rat cerebella, a preparation in which isolated GN actively migrate out of the tissue in the absence of cell to cell contacts (Yacubova and Komuro [2002a](#)), we first examined whether PACAP and components of the tPA-dependent proteolytic cascade can affect directly and independently GN migration. Application of PACAP (10⁻⁶ M) for 2 h significantly reduced GN motility by 70% (from 90 ± 5.4 μm/h to 27.3 ± 5.4 μm/h; Fig. [1](#)). Application of tPA (10⁻⁷ M) for 2 h did not alter GN velocity (79.2 ± 3.6 μm/h vs. 75.4 ± 7.3 μm/h; Fig. [2a](#)). Administration of plasminogen (a substrate of tPA; 10⁻⁷ M; 2 h) did not significantly modify GN motility (from 79.6 ± 1.6 μm/h vs. 68.8 ± 3.9 μm/h) (Fig. [2b](#)). Similarly, incubation of GN with PAI-1 (10⁻⁷ M), an inhibitor of tPA had no effect on cell motility (Fig. [2c](#)). Taken together, these results indicate that application of exogenous PACAP directly slows down the migration of rat GN, whereas members of the tPA-dependent proteolytic cascade do not exert a direct control of GN motility *in vitro*.

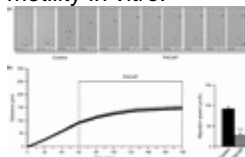


Figure 1. Pituitary adenylate cyclase-activating polypeptide (PACAP) slows down isolated cerebellar granule neurons (GN). (a) Time-lapse imaging showing the inhibitory effect of PACAP (10⁻⁶ M) on an

isolated GN escaping from a P4 cerebellum microexplant. After plating in glass bottom Petri dishes, GN were tracked by videomicroscopy for 1 h in control conditions and then for 2 h in the presence of PACAP. Asterisks mark the GN soma. Elapsed time (in min) is indicated at the bottom of each photomicrograph. Scale bar: 10 μm . (b) Sequential changes in the distance traveled by GN soma showing that PACAP (10^{-6} M) reduces GN movements immediately upon application. Results represent the mean \pm SEM (error bar) from $n = 44$ determinations. The histogram represents the change in the average migration speed after application of PACAP: *** $p < 0.001$ versus control.

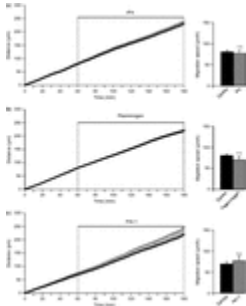


Figure 2. Members of the tissue-type plasminogen activator (tPA)-dependent proteolytic cascade have no effect on cerebellar granule neurons (GN) motility. (a–c) Sequential changes in the distance traveled by GN soma showing that tPA (10^{-7} M), plasminogen (10^{-7} M), and plasminogen activator inhibitor-1 (PAI-1) (10^{-7} M) do not affect the migration speed of GN. Results represent the mean \pm SEM (error bar) from $n = 88$, 114, and 65 determinations, respectively. The histograms compare the average migration speed of GN before and after application of tPA (a), plasminogen (b) and PAI-1 (c). n.s., not statistically significant versus control.

Distribution of tPA in cerebellar cortical layers of P10 rat

Previous reports have described the distribution of PACAP in the rat and mouse developing cerebellum by *in situ* hybridization and immunohistochemistry (Nielsen *et al.* [1998](#); Hannibal [2002](#); Cameron *et al.* [2007](#)). These studies have shown that PACAP is mainly expressed in the soma and dendrites of Purkinje cells and in mossy fiber terminals in the IGL (Cameron *et al.* [2007](#)). In contrast, the distribution of tPA in the developing cerebellum has only been investigated at the mRNA level (Friedman and Seeds [1995](#); Ware *et al.* [1995](#)). Therefore, we performed immunohistochemical staining with mouse polyclonal antibodies to localize endogenous tPA in the P10 rat cerebellum. Multi-labelings with the nuclear probe DAPI and with calbindin antibodies were also conducted to determine which cortical cerebellar layers (Fig. [3a](#)) and which cellular structures were tPA-positive. The EGL was virtually devoid of tPA immunoreactive signal (Fig. [3b–d](#)). In the ML, dendrites of Purkinje cells, surrounding DAPI-positive interneuron nuclei and the EM were moderately labeled with tPA antibodies (Fig. [3b–d](#)). Intense tPA-like immunoreactivity was observed in the PCL, the IGL, and the white matter (WM) of the cerebellum (Fig. [3b–d](#)). In the PCL, tPA-positive material was detected in the EM and in large soma of Purkinje cells (Fig. [3b–d](#)). Throughout the IGL, intense tPA

staining was seen in the EM and in most small DAPI-positive cell bodies (Fig. 3b-d). Collectively, these results indicate the existence of various endogenous sources of tPA and a cortical-layer-specific expression of tPA in the early post-natal rat cerebellum.

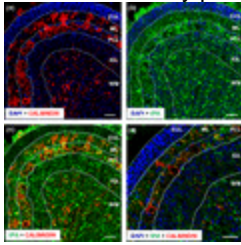


Figure 3. Tissue-type plasminogen activator (tPA) immunoreactivity is widely distributed in cortical layers of P10 rat cerebellum. (a–d) Immunohistochemical localization of tPA in the early post-natal cerebellum. Sagittal tissue sections from P10 rat cerebella were processed for tPA and calbindin immunohistochemistry as well as 4'6-diamidino-2-phenylindole (DAPI) labeling before confocal microscopy imaging. (a) Overlay of double labeling for calbindin-like immunoreactivity (red) and DAPI staining (blue) of nuclei allowing cortical layers demarcation and Purkinje cell localization. (b) Overlay of double labeling for tPA-like immunoreactivity (green) and DAPI showing large staining of the extracellular matrix and numerous positive small cell bodies in the molecular layer (ML) and the internal granular layer (IGL). (c) Overlay of double labeling for tPA- and calbindin-like immunoreactivity indicating that Purkinje cell soma and dendrites are positive for tPA. (d) Overlay of triple labeling for DAPI, calbindin-like and tPA-like immunoreactivity at higher magnification illustrating the presence of tPA in the interstitial space. Scale bar = 30 μm .

Effect of PACAP on centripetal migration of rat GN

To investigate whether PACAP affects the migration of rat granule cells in their natural microenvironment, P10 acute rat cerebellar tissue slices labeled with the CTG fluorescent dye were examined under a confocal microscope. Addition of exogenous PACAP38 (10^{-6} M) to the culture medium induced an immediate and strong decrease in the GN migration velocity in the ML (Fig. 4a). For example, the migration speed of GN in the ML, marked (*) and (#) in Fig. 4a, dropped from 14.5 $\mu\text{m}/\text{h}$ and 12.3 $\mu\text{m}/\text{h}$ in control conditions to 0.8 $\mu\text{m}/\text{h}$ and 6.4 $\mu\text{m}/\text{h}$ after application of 10^{-6} M PACAP38, respectively (Fig. 4b, c). Globally, the average migration speed of GN in the ML decreased from 9.1 ± 0.4 $\mu\text{m}/\text{h}$ ($n = 22$) in control conditions to 2.6 ± 0.2 $\mu\text{m}/\text{h}$ ($n = 44$) after PACAP treatment (Fig. 4d). Remarkably, PACAP38 (10^{-6} M) induced a 71% decrease in the migration speed of GN in the ML (Fig. 4d), and a 70% decrease in the migration speed in microexplants (Fig. 1b). These data indicate that the effect of exogenous PACAP on GN migration in slices was similar to that observed in microexplant cultures, which suggests that PACAP slows GN migration in the ML directly *via* activation of its receptors on the plasmalemmal surface of the cells. Previous studies have indicated that endogenous PACAP is responsible for the transient arrest phase of mouse GN in the PCL (Cameron *et al.* 2007). The potent PACAP antagonist, PACAP6-38, (Robberecht *et al.* 1992), was thus used to examine the role of endogenous PACAP38 in the control of GN migration in the PCL of early post-natal

rat cerebellum. Application of PACAP6-38 (10^{-6} M) to the culture medium increased the speed of GN migration by 23% at the level of the PCL (Fig. 4d), indicating that the slowdown of GN migration observed in the PCL of the early post-natal rat cerebellum is caused by endogenous PACAP38 through the activation of its receptors.

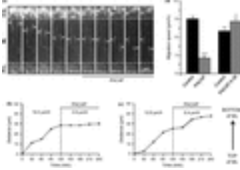


Figure 4. Endogenous pituitary adenylate cyclase-activating polypeptide (PACAP) reduces cerebellar granule neurons (GN) migration in P10 rat cerebellar slices. (a) Time-lapse imaging showing that exogenous PACAP (10^{-6} M) slows down GN movements in the molecular layer (ML). GN were tracked by confocal macroscopy for 2 h in control conditions and then for 2 h in the presence of PACAP. Asterisk (*) and sharp (#) symbols mark the GN soma. Elapsed time (in min) is indicated on the bottom of each photomicrograph. Scale bar = 10 μ m. (b–c) Sequential changes in the distance traveled by GN soma showing that exogenous PACAP (10^{-6} M) inhibits rapidly the migration of (*) and (#) marked GN. (d) Histogram showing that PACAP (10^{-6} M) reduces the average migration speed of GN in the ML, whereas the PACAP antagonist PACAP6-38 (10^{-6} M) increases the average migration speed of GN in the Purkinje cell layer (PCL). Results represent the mean \pm SEM (error bar) from $n = 66$ and $n = 36$ determinations, respectively. * $p < 0.05$; *** $p < 0.001$ versus control.

Effect of tPA on centripetal migration of rat GN

In the early post-natal cerebellum, granule cells exhibit significant changes in their migration speed as they cross different cortical layers (Komuro and Rakic 1995, 1998; Komuro *et al.* 2001; Komuro and Yacubova 2003; Kumada and Komuro 2004). The question was to know whether tPA could play a role in these cortical-layer-specific changes of GN velocity during their migration process. The average speed of GN as they migrate through the ML was 9.6 ± 0.9 μ m/h in control and 8.3 ± 0.9 μ m/h ($n = 20$) after addition of tPA (10^{-7} M) to the culture medium (Fig. 5a) indicating that exogenous tPA did not affect GN migration in the ML. In contrast, application of PAI-1, an inhibitor of endogenous tPA, inhibited GN migration in a layer-specific manner. Thus, PAI-1 (10^{-7} M) markedly slowed down GN migration in the ML (Fig. 5b). For example, the granule cell marked (*) in Fig. 5b reduced its migration speed in the ML from 14.2 μ m/h in control conditions to 2.7 μ m/h after addition of PAI-1 (Fig. 5c). Globally, in the presence of PAI-1 (10^{-7} M), the migration speed of granule cells was reduced by 70% in the ML and by 27% in the PCL, but stayed unchanged in the IGL (Fig. 5d). These results indicate that, in the early post-natal rat cerebellum, endogenous tPA participates to GN migration in the ML and PCL but not in the IGL, despite the fact that tPA is present in the three different layers.

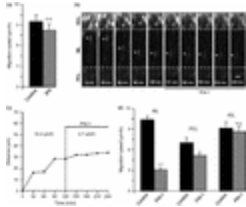


Figure 5. Endogenous tissue-type plasminogen activator (tPA) participates to cerebellar granule neurons (GN) migration in the molecular layer (ML) and Purkinje cell layer (PCL) of P10 rat cerebellar slices. (a) Histogram showing that exogenous tPA (10^{-7} M) does not affect the migration speed of GN in the ML. GN were tracked by confocal macroscopy for 2 h in control conditions and then for 2 h in the presence of tPA. (b) Time-lapse imaging showing the inhibitory effect of plasminogen activator inhibitor-1 (PAI-1) (10^{-7} M) on GN movements in the ML. GN were tracked by confocal macroscopy for 2 h in control conditions and then for 2 h in the presence of PAI-1. Asterisk marks the GN soma. Elapsed time (in min) is indicated on the bottom of each photomicrograph. Scale bar = 10 μ m. (c) Sequential changes in the distance traveled by GN soma showing that PAI-1 (10^{-7} M) immediately slows down GN migration in the ML. (d) Histogram showing that PAI-1 reduces the average migration speed of GN in the ML, the PCL but not in the internal granular layer (IGL). Results represent the mean \pm SEM from $n = 20$, $n = 96$, and $n = 32$ determinations, respectively. n.s., not statistically significant; * $p < 0.05$; *** $p < 0.001$ versus control.

Effect of tPA on centrifugal migration of rat B/SC

To investigate whether tPA and PACAP affect the centrifugal migration of rat basket/stellate cells in the ML, P10 rat cerebellar tissue slices labeled with the CTG fluorescent dye were examined under a confocal microscope (Fig. 6a). Although many B/SC were scattered throughout the ML, the density of CTG-labeled B/SC ($n = 306 \pm 79$ cell/ mm^2 of ML) is much lower than that of CTG-labeled GN ($n = 1124 \pm 138$ cell/ mm^2 of ML) (Fig. 6b). Most B/SC (90%; $n = 91$) migrate radially toward the top of the ML whereas only 10% ($n = 10$) migrate obliquely, reaching nevertheless the interface between the ML and the EGL (data not shown). Among B/SC that move radially in the ML, two types of migration speed profiles were observed in control conditions (Fig. 6c); that is 68% of the tracked cells had an average speed of 9.0 ± 0.4 $\mu\text{m}/\text{h}$ ($n = 65$) and were defined as slow cells, whereas 32% of the cells displayed a migration speed of 15.6 ± 0.5 $\mu\text{m}/\text{h}$ ($n = 26$) and were defined as fast cells. Both categories of cells had saltatory movements (Fig. 6d) and reached the top of the ML at the interface with the EGL. Following the same radial route, slow or fast B/SC intersect GN during their opposite migration in the ML (Fig. 7). After crossing a B/SC, GN often reduced their speed whereas the speed of B/SC was not affected by the presence of GN (Fig. 7a). B/SC can cross several GN (Fig. 7b) during their centrifugal move, suggesting that they share a common interneuron rail to guide their migration. Application of PACAP6-38 (10^{-6} M) did not significantly affect the average speed of slow (8.1 ± 0.4 $\mu\text{m}/\text{h}$; $n = 25$) and fast (16 ± 1.1 $\mu\text{m}/\text{h}$; $n = 7$) B/SC nor their proportion (76% and 24%) (Fig. 8a), suggesting that endogenous PACAP does not interfere with B/SC migration in the ML. In contrast, PAI-1

(10^{-7} M) increased to 94% ($n = 68$) the proportion of slow migrating cells, so that only a few fast B/SC could still be observed (6%; $n = 7$) (Fig. 8a). Treatment with PAI-1 (10^{-7} M) did not affect the migration of slow BS/C in the ML. For example, the migration speed of slow BS/C in the ML was similar in control conditions (10.3 $\mu\text{m}/\text{h}$) or after application of tPA (10^{-7} M; 11.6 $\mu\text{m}/\text{h}$; Fig. 8b) whereas PAI-1 (10^{-7} M) strongly reduced the migration speed of fast BS/C in the ML from 16.8 $\mu\text{m}/\text{h}$ in control conditions to 7.3 $\mu\text{m}/\text{h}$ (Fig. 8c).

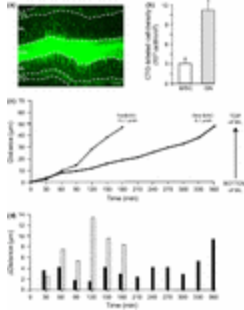


Figure 6. Migrating basket/stellate cells (B/SC) exhibit two types of speed profiles in the molecular layer (ML). (a) Macroconfocal view of a P10 rat cerebellar slice in which cell tracker green (CTG)-labeled B/SC and cerebellar granule neurons (GN) are tracked every 30 min. Scale bar = 50 μm . (b) Histogram showing the low density of B/SC compared to the high density of GN in the ML. (c) Sequential changes in the distance traveled by B/SC soma showing that fast and slow cells can be identified in the ML. (d) Distance traveled by slow (black histograms) and fast (dotted-line histograms) B/SC during each 30-min acquisition period, illustrating the saltatory movements of both types of cells.

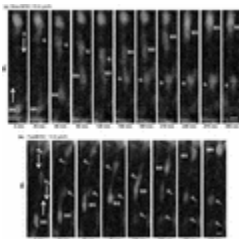


Figure 7. Basket/stellate cells (B/SC) and cerebellar granule neurons (GN) use common rail of migration in the molecular layer (ML). (a–b) Time-lapse imaging showing intersection of slow (a) and fast (b) B/SC with GN. BS and G_a/G_b mark B/SC and GN soma, respectively. Bottom-up and top-down arrows indicate centrifugal and centripetal migration, respectively. Elapsed time (in min) is indicated under each photomicrograph. Scale bar = 5 μm .

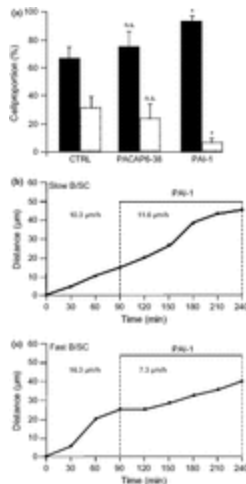


Figure 8. Tissue-type plasminogen activator (tPA) participates to the control of migration of fast basket/stellate cells (B/SC), whereas pituitary adenylate cyclase-activating polypeptide (PACAP) has no effect on any B/SC. (a) Histogram showing that blockage of endogenous PACAP by the PACAP antagonist PACAP6-38 (10^{-6} M) has no effect on the proportion of slow (black histogram) and fast (dotted-line histogram) B/SC, whereas blockade of endogenous tPA with plasminogen activator inhibitor-1 (PAI-1) markedly decreases the proportion of fast B/SC. (b) Sequential changes in the distance traveled by slow B/SC soma showing that PAI-1 (10^{-7} M) does not significantly modify the migration speed of slow cells in the molecular layer (ML). (c) Sequential changes in the distance traveled by fast B/SC soma showing that PAI-1 (10^{-7} M) strongly slows down the migration of fast cells in the ML. Results represent the mean \pm SEM from $n = 91$ (control), $n = 32$ [PACAP(6-38)] and $n = 75$ (PAI-1) determinations, respectively. n.s., not statistically significant; * $p < 0.05$ versus control.

Discussion

The cerebellar cortex of rodents undergoes major changes during the first four post-natal weeks (Altman and Bayer [1997](#)). Excitatory (GN) and inhibitory (B/SC) interneurons, with distinct embryological origins and opposite migration directions, populate the IGL and the ML, respectively, between P0 and P21 and control Purkinje cell activities in adult (Consalez and Hawkes [2013](#)). Here, we report for the first time the direct inhibitory effect of PACAP on GN movements and the facilitatory role of the serine protease tPA on both GN and fast B/SC migration in specific cortical cell layers of the developing rat cerebellum.

Using microexplant cultures, this study revealed that application of exogenous PACAP reduces by 70% the migration speed of rat GN, whereas tPA, plasminogen (a tPA substrate) or PAI-1 (a tPA inhibitor) do not alter GN motility *in vitro*. We have previously shown that PACAP stimulates tPA release from GN and that the inhibitory effect of PACAP on rat GN movement is not affected by PAI-1 or plasminogen pre-incubation (Raoult *et al.* [2011](#)). Altogether, these data indicate that PACAP exerts a direct inhibitory effect on rat GN, whereas tPA, and probably PACAP-induced tPA release, is likely to promote indirectly neuronal migration

through proteolytic degradation of the EM. In support of this hypothesis, tPA is concentrated in leading processes of mouse GN during cerebellar development (Krystosek and Seeds [1981a,b](#); Seeds *et al.* [1997](#)) where it facilitates GN migration (Seeds *et al.* [1999](#)).

While the distribution pattern of PACAP in the post-natal cerebellum is now well established (Nielsen *et al.* [1998](#); Hannibal [2002](#); Cameron *et al.* [2007](#)), the localization of the tPA protein is still unknown as the cellular expression of tPA has only been investigated by *in situ* hybridization experiments (Friedman and Seeds [1995](#); Ware *et al.* [1995](#)). This study revealed that tPA-like immunoreactivity is widely distributed in the ML, the PCL, the IGL, and the WM of the cerebellum of P10 rats. In contrast, the EGL was virtually devoid of immunoreactive signal. The intense labeling observed in the EM in the different cortical layers of the cerebellum strengthens the possible contribution of tPA in the control of neuronal migration through its proteolytic activity. Several cell types could be the source of tPA since Purkinje cells and numerous small cell bodies, including possibly granule cells, were immunolabeled. The distribution of tPA-immunoreactive material is consistent with previous studies indicating the presence of tPA mRNA at the level of Purkinje cells and GN, but also in the IGL and the WM, during cerebellar development (Friedman and Seeds [1995](#); Ware *et al.* [1995](#)). The detection of PACAP and tPA along the migratory routes of interneurons through the ML, PCL, and IGL strongly suggested important roles for both factors in the control of GN and B/SC movements. To test this hypothesis, we have investigated the effect of PACAP, tPA, and PACAP-induced tPA release on interneuron migration in cerebellar slices, in which the cytoarchitecture remains intact, to study the proteolytic activity of tPA.

Time-lapse macroconfocal experiments revealed that exogenous PACAP38 slows down by 71% centripetal GN migration in the ML, whereas the PACAP antagonist PACAP6-38 increases the speed of GN migration by 23% in the PCL. These results confirmed, *ex vivo*, the direct inhibitory effect of PACAP on rat GN migration observed *in vitro* and suggest that the decrease in speed of GN at the level of the PCL in the developing post-natal rat cerebellum is caused by endogenous PACAP through the activation of its G-protein-coupled receptor via cAMP- and Ca²⁺-dependent mechanisms as observed in mouse (Cameron *et al.* [2007](#), [2009a](#)). Previous studies have revealed the contribution of tPA on GN migration in the ML of tPA^{-/-} mice (Seeds *et al.* [1999](#)), but the role of tPA in the PCL and the IGL had never been investigated. Using the model of cerebellar tissue slices, time-lapse macroconfocal imaging revealed that exogenous tPA does not alter GN migration in the ML, whereas PAI-1 reduces the velocity of GN by 70% in the ML and by 27% in the PCL but has no effect in the IGL. Altogether, these data indicate that, in the early post-natal rat cerebellum, tPA favors GN migration not only in the ML as previously described (Seeds *et al.* [1999](#)) but also in the PCL. Thus, we have shown that endogenous tPA contributes to the glia-dependent radial migration of GN in the ML and to the glia-independent radial migration of GN in the PCL. As both PACAP and tPA have been found to be involved in cell migration within the PCL, we suggest that the stimulatory effect of PACAP on tPA secretion from GN, previously reported *in vitro* (Raoult *et al.* [2011](#)), takes place at the level of the PCL and that this secretion of tPA induced by PACAP could contribute to the

resumption of GN migration toward the IGL after their transient arrest at the level of the PCL. During post-natal development of the cerebellum, this pause of GN is well established but its functional significance remains unknown. Transient arrest phases of various duration appear to be a frequent feature of neuronal migration in brain histogenesis (Noctor *et al.* [2004](#)). For instance, pyramidal neurons stop their migration for 24 h in the intermediate zone before attaining the cortical plate (Kriegstein and Noctor [2004](#)). GABAergic interneurons first reach the ventricular zone of the cortex where they stay for a short time (45 min) and receive layer information that are essential for their final migration toward the cortical plate (Nadarajah *et al.* [2002](#)). As PACAP is involved in neurogenesis (Gonzalez *et al.* [1997](#); Falluel-Morel *et al.* [2005](#)), the transient arrest phase could be necessary for the initiation of a differentiation program and/or for a correct integration of GN in the IGL. As an example, somatostatin is the stop signal for GN in the IGL, but the subtype of receptor that mediates the inhibitory effect on GN migration is still a matter of debate (Viollet *et al.* [1997](#); Yacubova and Komuro [2002b](#)). In fact, somatostatin stimulates the tangential migration of GN in the EGL through sst2 receptors but exerts an opposite effect in the IGL through a different type of receptor. Thus, PACAP could be responsible for the switch of somatostatinergic control of GN migration by stimulating the recruitment and/or expression of new sst receptor subtype(s) or by modulating their transduction mechanisms (Goth *et al.* [1992](#)). In the IGL, endogenous PACAP and tPA do not regulate the glia-independent radial migration of GN but are likely to play a neurotrophic action. Previous studies have shown that GN, without proper trophic support from glutamatergic mossy fibers, die by apoptosis in the IGL (Williams and Herrup [1988](#); Wood *et al.* [1993](#)). PACAP, that is contained in mossy fibers (Cameron *et al.* [2007](#)), promotes *in vitro* GN survival through the release of tPA (Raoult *et al.* [2011](#)). In addition, the thickness of the IGL is significantly reduced at P7 in PACAP-knockout (PACAP^{-/-}) mice (Allais *et al.* [2007](#)). Taken together, these data strongly suggest the contribution of PACAP-induced tPA secretion to the neuroprotective effect of PACAP in the IGL.

While GN migrate from the EGL toward the IGL, basket and stellate cells migrate from the WM to reach the inferior or superior part of the ML, respectively (Rakic [1973](#); Zhang and Goldman [1996](#); Yamanaka *et al.* [2004](#); Leto *et al.* [2006](#); Cameron *et al.* [2009b](#)). In this study, we referred to basket cells and stellate cells as immature B/SC, and analyzed their radial centrifugal migration in the ML as a single-cell type because they are morphologically indistinguishable (Cameron *et al.* [2009b](#)). However, we cannot rule out the possibility that basket cells and stellate cells exhibit some differences in their speed and regulation of migration. In the P10 ML, we have determined the low density of migrating labeled B/SC compared to GN density. As in mouse (Cameron *et al.* [2009b](#)), a large majority (90%) of BS/C displayed a radial migration, whereas only 10% of the cells migrated obliquely toward the top of the ML. In the ML, two types of B/SC have been identified for the first time according to their radial migration speed and designated as slow (68%) and fast (32%) cells. Both slow and fast cells reached the top of the ML with saltatory movements as previously described in mouse (Cameron *et al.* [2009b](#)). As a new concept in cerebellar interneuron migration, we have shown that slow and fast BS/C intersect with GN, suggesting that they share a common

migratory rail in the ML and that some GN tend to slow down after crossing B/SC. In the presence of PAI-1, 94% of B/SC exhibited a slow profile, indicating that endogenous tPA participates to the radial centrifugal migration of fast cells, whereas the migration of slow cells is independent of tPA. Both Purkinje cells and GN (Friedman and Seeds [1995](#); Raoult *et al.* [2011](#); this study) express tPA and could therefore release tPA in the EM to facilitate the migration of fast cells. Several hypotheses have been proposed for B/SC guiding along the migration routes. B/SC movements could be facilitated along GN axons as well as Purkinje cell axons, climbing fibers and mossy fibers through cell to cell contacts (Guijarro *et al.* [2006](#); Cameron *et al.* [2009b](#)). As radial centripetal migration of GN in the ML depends on both tPA (Seeds *et al.* [1999](#); this study) and glial fibers (Komuro and Rakic [1998](#)), Bergmann glial processes may also serve as a scaffold for radial migration of B/SC in the ML through a tPA-dependent mechanism. Whether differences in the speed and regulation of migration discriminate slow and fast cells as basket and stellate cells or *vice versa* is still a matter of debate since subtypes of basket and/or stellate cells may also exist (Consalez and Hawkes [2013](#)).

At the top of the ML, a high density of immature B/SC has been described suggesting that they sojourn next to the EGL before they ultimately translocate to the middle part of the ML (Weisheit *et al.* [2006](#)) and that this is a necessary step for their differentiation and proper distribution. At present, little is known regarding the possible regulators of BS/C migration except that inhibitory interneurons display repulsive behavior against Netrin1 which is abundant in the EGL during the early post-natal period (Alcantara *et al.* [2000](#); Guijarro *et al.* [2006](#)). Here, we show that PACAP does not affect the radial centrifugal migration of B/SC in the ML. The observation that PACAP6-38 had no effect on B/SC migration indicates that tPA-induced promotion of fast cell movement is also independent of PACAP. PACAP usually exerts dual effects on neural/glial cells that is, inhibition of migration and stimulation of differentiation. Consistent with this notion, the PACAP/PAC1 (PACAP receptor type 1) system promotes stellate morphology in astrocytes (Nishimoto *et al.* [2007](#)). PACAP could therefore be involved in the completion of B/SC migration in the middle of the ML, where inhibitory interneurons extend dendrite-like processes (Cameron *et al.* [2009b](#)). Interestingly, B/SC did not stop in the PCL in contrast to GN that exhibit a PACAP-dependent arrest phase of approximately 2 h (Cameron *et al.* [2007](#), [2009b](#)). This suggests that GN and B/SC require, along their migratory route, a cortical-layer-specific 'stand by' phase before their correct and final integration. This pause phase would be necessary for the initiation of intrinsic programs that may control expression of the receptors which recognize final external stop signals or initiate the differentiation program.

In conclusion, our data indicate for the first time that, during the second post-natal week in the rat cerebellum, GN and B/SC migrate radially along Bergmann fibers but in opposite directions, crossing each other in the ML. In the ML, through degradation of the EM, tPA exerts a central role facilitating centripetal and centrifugal migration of GN and fast B/SC, respectively. PACAP is responsible for the transient arrest phase of migrating GN in the PCL, and PACAP-induced tPA release could therefore stimulate the resumption of GN migration to reach their final position in the IGL.



Acknowledgements and conflict of interest disclosure

This work was supported by the Institute for Research and Innovation in Biomedicine (IRIB), the Cell Imaging Platform of Normandy (PRIMACEN), INSERM, the FEDER (# 2517), Interreg 4A TC2N European project, the LARC-Neurosciences Network, and the Région Haute-Normandie. E.R. was the recipient of a doctoral fellowship from the LARC-Neuroscience Network and the Région Haute-Normandie. D.V. and H.V. are Affiliated Professors at the Institut National de la Recherche Scientifique – Institut Armand-Frappier. The authors have no conflict of interest to declare.